DALTON

Synthesis, properties, stereochemistry and crystal structures of diastereomeric benzene–ruthenium(II) complexes with a chiral salicylideneaminato ligand†

Henri Brunner,*[a] Ralf Oeschey[a] and Bernd Nuber[b]

[a] *Institut für Anorganische Chemie der Universität Regensburg, Universitätsstrasse 31, D-93053 Regensburg, Germany*

[b] *Anorganisch-Chemisches Institut der Universität Heidelberg, Im Neuenheimer Feld 270, D-69120 Heidelberg, Germany*

The reaction of $[\{Ru(\eta^6\text{-}C_6H_6)Cl_2\}_2]$ with the sodium salt of (*S*)-*N*-(1-phenylethyl)salicylideneamine (HL–L) in CH_2Cl_2 led to a diastereomer mixture of (R_{Ru},S_C)- and (S_{Ru},S_C)-$[Ru(\eta^6\text{-}C_6H_6)(L\text{–}L)Cl]$ **1a** and **1b**, in a ratio of 86:14. Mediated by $AgPF_6$ in acetone at −30 to −35 °C, the chloride ligand in **1a**/**1b** was substituted by 4-methylpyridine (4Me-py), 2-methylpyridine (2Me-py) or triphenylphosphane (PPh_3) to give the two diastereomers **2a**/**2b** of $[Ru(\eta^6\text{-}C_6H_6)(L\text{–}L)(4Me\text{-}py)]PF_6$, the pure diastereomer **3** of $[Ru(\eta^6\text{-}C_6H_6)(L\text{–}L)(2Me\text{-}py)]PF_6$ and the two diastereomers **4a**/**4b** of $[Ru(\eta^6\text{-}C_6H_6)(L\text{–}L)(PPh_3)]PF_6$. At room temperature in $[^2H_6]$acetone, under equilibrium conditions, the diastereomer ratio **2a**:**2b** was 67:33, **3** was diastereomerically pure and the ratio **4a**:**4b** was 93.4:6.6. Variable-temperature ^1H NMR spectroscopy of complexes **2a**/**2b** and **4a**/**4b** from −80 °C to room temperature demonstrated configurational lability of the ruthenium configuration. Since equilibration occurred during reaction and work-up, the ruthenium configuration was not retained in the substitution reactions. Diastereomer **2a** was obtained diastereomerically pure by crystallisation. The diastereomers **4a** and **4b** were separated and examined by variable-temperature NMR spectroscopy. The crystal structures of the (R_{Ru},S_C) diastereomer of complex **1** and of the thermodynamically more stable (R_{Ru},S_C) diastereomers **2a** and **4a**″ were determined by X-ray analysis. A conformational analysis based on the NMR spectroscopic results showed that two main factors govern the orientation of the 1-phenylethyl group relative to the $[Ru(\eta^6\text{-}C_6H_6)(L\text{–}L)L']$ moiety (L′ = Cl, 4Me-py, 2Me-py or PPh_3): (*i*) the face-on orientation of the phenyl substituent with respect to the π-bonded aromatic benzene ligand and (*ii*) the steric demand of the unidentate ligands with respect to the 1-phenylethyl group.

The elucidation of the stereochemistry of reactions of optically active transition-metal complexes should be revealing in terms of the mechanisms of chirality transfer in enantioselective catalysis. Cyclopentadienyl transition-metal half-sandwich complexes, in particular ruthenium compounds, have been intensely studied.[2,3] Arene-ruthenium(II) complexes have aroused interest owing to their catalytic potential.[4] Recently, preparative and stereochemical studies on (η^6-*p*-cymene)ruthenium(II) complexes with (*S*)-*N*-(1-phenylethyl)salicylideneaminate (L–L) as a chiral chelating ligand and various monodentate ligands were published in this and other journals.[5a–c] Since some of the experimental results and conclusions in these papers are definitely wrong we set out to rectify them.[6]

In this paper we report on the synthesis, NMR spectroscopic and chiroptical properties of $[Ru(\eta^6\text{-}C_6H_6)(L\text{–}L)Cl]$ **1** and chloride-substituted derivatives. The crystal structures of three diastereomers were determined. Where appropriate, wrong conclusions[5] are corrected in the text. A preliminary communication[7] containing part of our investigations and a note[1] with regard to the previous publications[5] have been published.

Experimental

Physical measurements and materials

Reactions were carried out under a nitrogen atmosphere using the Schlenk technique. Cyclohexa-1,3-diene was obtained from Janssen Chimica (now Acros Chimica), $RuCl_3 \cdot xH_2O$ from Hereaus and as a donation from Degussa, triphenylphosphane, 4- and 2-methylpyridine from Fluka, and $AgPF_6$ from Johnson Matthey. The compounds $[\{Ru(\eta^6\text{-}C_6H_6)Cl_2\}_2]$[8] and (*S*)-(+)-*N*-(1-phenylethyl)salicylideneamine[9] were prepared by the literature methods. (*S*)-1-phenylethylamine was a gift from BASF.

Elemental analyses were performed by the microanalytical laboratory of the University of Regensburg. Mass spectra were recorded with a Finnigan MAT 95 instrument by the field-desorption (FD) method, ^1H NMR spectra with tetramethylsilane as internal standard on Bruker AC 250 and ARX 400 spectrometers. With the latter, $^{13}C\text{-}\{^1H\}$ and $^{31}P\text{-}\{^1H\}$ (85% H_3PO_4 as external standard) NMR spectra were measured. Circular dichroism (CD) spectra were recorded with a JASCO J-40 A spectrophotometer, and polarimetric measurements were carried out with a Perkin-Elmer 241 instrument.

Preparations

$[Ru(\eta^6\text{-}C_6H_6)(L\text{–}L)Cl]$ 1. Sodium hydride (163 mg, 6.79 mmol) was suspended in CH_2Cl_2 (15 cm^3). A solution of HL–L (1.53 g, 6.79 mmol) in CH_2Cl_2 (20 cm^3) was added at 0 °C. When hydrogen evolution had ceased, $[\{Ru(\eta^6\text{-}C_6H_6)Cl_2\}_2]$ (1.54 g, 3.09 mmol) and CH_2Cl_2 (45 cm^3) were added. After stirring for 2 h at 0–5 °C the dark red solution was filtered through Celite and evaporated to dryness. The reddish residue was washed twice with acetone–light petroleum (b.p. 40–60 °C) (1:8), dried and dissolved in CH_2Cl_2 (15 cm^3). Upon addition of acetone (30 cm^3) and light petroleum (90 cm^3), crystallisation immediately set in and was completed overnight at −30 °C. The red-violet, air-stable crystals, suitable for X-ray analysis, were washed several times with acetone–light petroleum (1:1 to 1:5) and dried. Yield 2.03 g (4.63 mmol, 75%), m.p. 206–208 °C

† Optically Active Transition Metal Complexes. Part 107.[1]

(decomp.) (Found: C, 57.50; H, 4.65; N, 3.25. Calc. for $C_{21}H_{20}ClNORu$: C, 57.45; H, 4.60; N, 3.20%). FD mass spectrum (CH_2Cl_2): *m/z* 439.4 ($[M]^+$, 100) and 404.3 ($[M - Cl]^+$, 1%), referred to ^{102}Ru. In $CDCl_3$ and CD_2Cl_2 solution the product exhibits ^1H NMR signals for two diastereomers in an 86:14 ratio, determined by integration of the signals of the η^6-benzene ligand (Table 2). The following chiroptical properties refer to the diastereomer mixture. $[\alpha]^{22}$ ($= 100\alpha/lc$, where α is the observed rotation in degrees, l is the path length in dm and c is the concentration in g per 100 cm^3 solution) (c = 0.4, CH_2Cl_2): (589) 279, (578) −317 and (546 nm) −475. CD data ($c = 9.57 \times 10^{-4}$ mol dm^{-3}, 22 °C, CH_2Cl_2): $\lambda_{max}(\Delta\varepsilon/dm^3$ mol^{-1} cm^{-1}) 305 (6.0), 375 (−10.8), 445 (−4.5), 530 (0.4); λ_0 329, 512 nm.

[Ru(η^6-C_6H_6)(L–L)(4Me-py)]PF_6 2. (4Me-py = 4-methylpyridine). The diastereomer mixture **1a/1b** (177 mg, 0.40 mmol) was suspended in acetone (30 cm^3) at −30 °C. Addition of $AgPF_6$ (103 mg, 0.40 mmol) resulted in a red-orange solution and precipitated AgCl. After stirring for 1 h at −30 °C, 4-methylpyridine (0.059 cm^3, 57 mg, 0.60 mmol) was added. Stirring the mixture for 30 min and filtration through Celite gave a yellow-orange solution. The solvent was removed and the residue was washed with light petroleum. The yellow solid was recrystallised from acetone–hexane (11:5). Yield 223–235 mg (0.35–0.37 mmol, 87–92%) of red-orange plates, suitable for X-ray analysis, m.p. 210–212 °C (decomp.) (Found: C, 50.65; H, 4.15; N, 4.45. Calc. for $C_{27}H_{27}F_6N_2OPRu$: C, 50.55; H, 4.25; N, 4.35%). FD mass spectrum (CH_2Cl_2): *m/z* 404.2 (cation − 4Me-py, 100%), referred to ^{102}Ru. At room temperature in $[^2H_6]$acetone solution the product exhibits ^1H NMR signals for two diastereomers in a 67:33 ratio, while in $CDCl_3$ a ratio of 86:14 was found. The chiroptical properties refer to the 67:33 diastereomer mixture. $[\alpha]^{22}$ (c = 0.4, acetone): (589) +47, (578) +78 and (546 nm) +249. CD data ($c = 6.36 \times 10^{-4}$ mol dm^{-3}, 22 °C, CH_2Cl_2): $\lambda_{max}(\Delta\varepsilon/dm^3$ mol^{-1} cm^{-1}); 285 (4.7), 320 (−9.4), 402 (−17.0) and 457 (10.6); λ_0 296, 432 nm.

[Ru(η^6-C_6H_6)(L–L)(2Me-py)]PF_6 3. Complex **3** was prepared in the same manner as **2** and recrystallised from acetone–hexane (10:9) at −25 °C. Yield 92% of red, prismatic crystals, m.p. 205–208 °C (decomp.) (Found: C, 50.30; H, 4.15; N, 4.35. Calc. for $C_{27}H_{27}F_6N_2OPRu$: C, 50.55; H, 4.25; N, 4.35%). At room temperature in $[^2H_6]$acetone solution the product exhibits ^1H NMR signals for only one diastereomer. Therefore the chiroptical properties refer to the pure diastereomer. $[\alpha]^{22}$ (c = 0.4, acetone): (589) +505, (578) +631 and (546 nm) +1242. CD data ($c = 6.36 \times 10^{-4}$ mol dm^{-3}, 22 °C, CH_2Cl_2): $\lambda_{max}(\Delta\varepsilon/dm^3$ mol^{-1} cm^{-1}); 313 (−21.0), 365 (−15.4), 405 (−20.9) and 475 (21.0); λ_0 436 nm. The crystals transformed into powder without decomposition at room temperature.

(R_{Ru},S_C,M_{PPh_3})-, (R_{Ru},S_C,P_{PPh_3})- and (S_{Ru},S_C)-[Ru(η^6-C_6H_6)(L–L)(PPh_3)]PF_6 4a, 4a′ and 4b. The synthesis of the mixture of isomers **4a**, **4a′** and **4b** and the isolation and characterisation of **4a** and **4a′** with different triphenylphosphane helicities but the same (R_{Ru},S_C) configuration was described previously.[7] The isolation of the thermodynamically unstable diastereomer **4b** with (S_{Ru},S_C) configuration was achieved as follows. The diastereomer mixture **1a/1b** (745 mg, 1.70 mmol) and PPh_3 (534 mg, 2.04 mmol) were dissolved in CH_2Cl_2 (120 cm^3). Silver hexafluorophosphate (429 mg, 1.70 mmol) was added to the red solution at −35 °C, which was stirred for 2 h at −30 to −35 °C. After cooling to −50 to −60 °C the precipitated AgCl was filtered off through Celite. The solution was concentrated below −30 °C to approximately half its volume. Then while stirring, light petroleum at −50 °C was added about five times in portions of 5–10 cm^3 and then twelve times in portions of about 10–15 cm^3 until complete precipitation had occurred. After decantation, the resulting orange precipitate was dried (yield 99%, analytically pure, ^1H NMR spectroscopy in $[^2H_6]$acetone at −50 °C shows **4a** and **4b** in a 1:1 ratio). The microcrystalline powder was stirred for 30 min with $CHCl_3$ (60 cm^3) at −60 °C. The suspension was then filtered through Celite and the insoluble residue washed twice with cold $CHCl_3$ (*ca.* 10 cm^3). From the filtrate, complexes **4a** and **4a′** can be obtained after precipitation as described.[7] FD mass spectrum of **4a** (CH_2Cl_2): *m/z* 666.7 (cation, 100) and 404.3 (cation − PPh_3, 27%), referred to ^{102}Ru. δ_P(162 MHz, $[^2H_6]$acetone, −45 °C) −142.7 (1 P, spt, $^1J_{PF}$ 708 Hz, PF_6) and 37.2 (1 P, s, PPh_3). $[\alpha]^{-18}$ (c = 0.08, CH_2Cl_2): (589) −1076, (578) −1276 and (546 nm) −2072. CD data ($c = 2.34 \times 10^{-4}$ mol dm^{-3}, −21 °C, CH_2Cl_2): λ_{max} ($\Delta\varepsilon/dm^3$ mol^{-1} cm^{-1}) 286 (3.1), 304 (5.2), 352 (−5.8), 393 (12.2) and 443 (−14.5); λ_0 327, 369 and 414 nm. The residue after filtration was dissolved in CH_2Cl_2 (100–150 cm^3) at −60 °C. Diastereomer **4b** was precipitated at −35 °C by slow addition of cold light petroleum (200 cm^3) in portions of about 10 cm^3. Decantation and drying gave an orange powder, almost insoluble in $CHCl_3$ and relatively stable towards air at room temperature. Yield 462 mg (0.57 mmol, 67% with respect to the 1:1 diastereomer mixture **4a/4b**), m.p. 205–206 °C (decomp.) (Found: C, 57.45; H, 4.70; N, 1.95. Calc. for $C_{39}H_{35}F_6NOP_2Ru$: C, 57.80; H, 4.35; N, 1.75%). ^1H NMR spectroscopy at variable temperature (range −80 to −20 °C) in $[^2H_6]$acetone showed that **4b** was more than 99% diastereomerically pure. δ_P(162 MHz, $[^2H_6]$acetone, −80 °C) −142.7 (1 P, spt, $^1J_{PF}$ 709 Hz, PF_6) and 28.3 (1 P, s, PPh_3). $[\alpha]^{-35}$ (c = 0.08, CH_2Cl_2): (589) −92, (578) −86 and (546 nm) −27. CD data ($c = 3.21 \times 10^{-4}$ mol dm^{-3}, −35 °C, CH_2Cl_2): $\lambda_{max}(\Delta\varepsilon/dm^3$ mol^{-1} cm^{-1}) 350 (8.7), 395 (−19.5), 438 (6.8) and 548 (−0.3); λ_0 315, 370, 423 and 525 nm. Crystallisation of **4b** (390 mg, 0.48 mmol) from CH_2Cl_2–light petroleum (8:5) at −20 to 3 °C (cooling bath warmed up in 63 h) resulted in the formation of red, prismatic crystals of **4a″**, suitable for X-ray analysis. Yield: 50 mg (0.06 mmol, 12%). The ^1H NMR spectrum at −80 °C in $[^2H_6]$acetone was identical with that of **4a** and **4a′**, respectively, except the signal due to crystal-bound CH_2Cl_2.

Crystallography

The details of the crystal structure determinations are summarised in Table 1. All structures were solved using a combination of Patterson–Fourier and least-squares methods.

Data collection for complexes 1a, 2a and 4a″. Cell constants for the three complexes were obtained from least-squares refinement of the setting angles of 25, 27 and 24 centred reflections in the ranges $4.0 < 2\theta < 26.0$, $6.0 < 2\theta < 33.0$ and $4.0 < 2\theta < 25.0°$, respectively. The data were collected in the ω-scan mode and in all cases three standard reflections were measured every 100. No profound loss of intensity was observed. The data were corrected for Lorentz and polarisation factors.

Structure solution and refinement. *Complexes* **1a** *and* **4a″**. The absolute configurations were determined by refinement of the least-squares variable η [= 0.9(1) for **1a**, −1.3(3) for **4a″** with the assumption of a (S_{Ru},R_C) configuration].[10,11] Hydrogen atoms were added in calculated positions with the option HFIX of the SHELXTL PLUS program package.[10] They were included in structure-factor calculations but not refined. Neutral atom scattering factors were used.[12]

Complex **2a.** The crystal which is assigned to the monoclinic system was measured in the range $3.0 < 2\theta < 55.5°$ as belonging to the triclinic system in order to obtain the Friedel pairs. With the latter the absolute configuration was determined. The refinement of the least-squares variable η for a (S_{Ru},R_C) configuration gave a value of −1.0(1).[10,11] The

subsequent procedure was as described for complexes **1a** and **4a**″.

Further details of the crystal structure determinations can be requested from the Gesellschaft für wissenschaftlich-technische Informationens, Fachinformationszentrum Karlsruhe, D-76344 Eggenstein-Leopoldshafen, Germany, under the deposit number CSD-59145. See Instructions for Authors, *J. Chem. Soc., Dalton Transactions*, 1996, Issue 1.

Results and Discussion

Synthesis and characterisation of complexes 1a/1b

The reaction of the dimeric complex $[\{Ru(\eta^6\text{-}C_6H_6)Cl_2\}_2]$ with the sodium salt of the chiral Schiff base (*S*)-*N*-(1-phenylethyl) salicylideneamine, in CH_2Cl_2 at 0 °C results in the formation of a diastereomer mixture of $[Ru(\eta^6\text{-}C_6H_6)(L\text{–}L)Cl]$ **1a/1b** (Scheme 1). Crystallisation of the mixture gave air-stable, red-violet plates of **1a**, suitable for X-ray analysis (see below). Solutions of these crystals in $CDCl_3$ as well as of the mixture obtained before crystallisation exhibit at room temperature in the ^1H NMR spectrum the signals of both diastereomers **1a** and **1b** in a ratio of 86:14 (Table 2). A sample of the crystals of **1a** dissolved in CD_2Cl_2 at −80 °C and measured at this temperature showed the same diastereomer ratio of 86:14 as at room temperature. The major diastereomer **1a** is characterised by the high-field signal at δ 5.31 of the η^6-benzene ligand. The low-field signal at δ 5.45 corresponds to the minor diastereomer **1b**. The diastereomer ratio is nearly the same as for the corresponding η^6-*p*-cymene complexes.[5]

Crystal structure of complex 1a

An X-ray analysis was performed for one of the crystals of complex **1a**. There are four independent molecules in the unit cell, all of them with the same configuration. In Fig. 1 an ORTEP[13] view of one of the molecules is shown. Details of the data collection and structure refinement are given in Table 1. Atomic coordinates and selected bond distances and angles in Tables 3 and 4, respectively. The chiral carbon atom of the chelate ligand has the expected (S_C) configuration, while the stereogenic ruthenium centre has the (R_{Ru}) configuration, specified with the priority sequence $\eta^6\text{-}C_6H_6$ > Cl > O (L–L) > N (L–L).[14]

Two independent single crystals of the same sample of complex **1** showed the same unit-cell parameters and all the

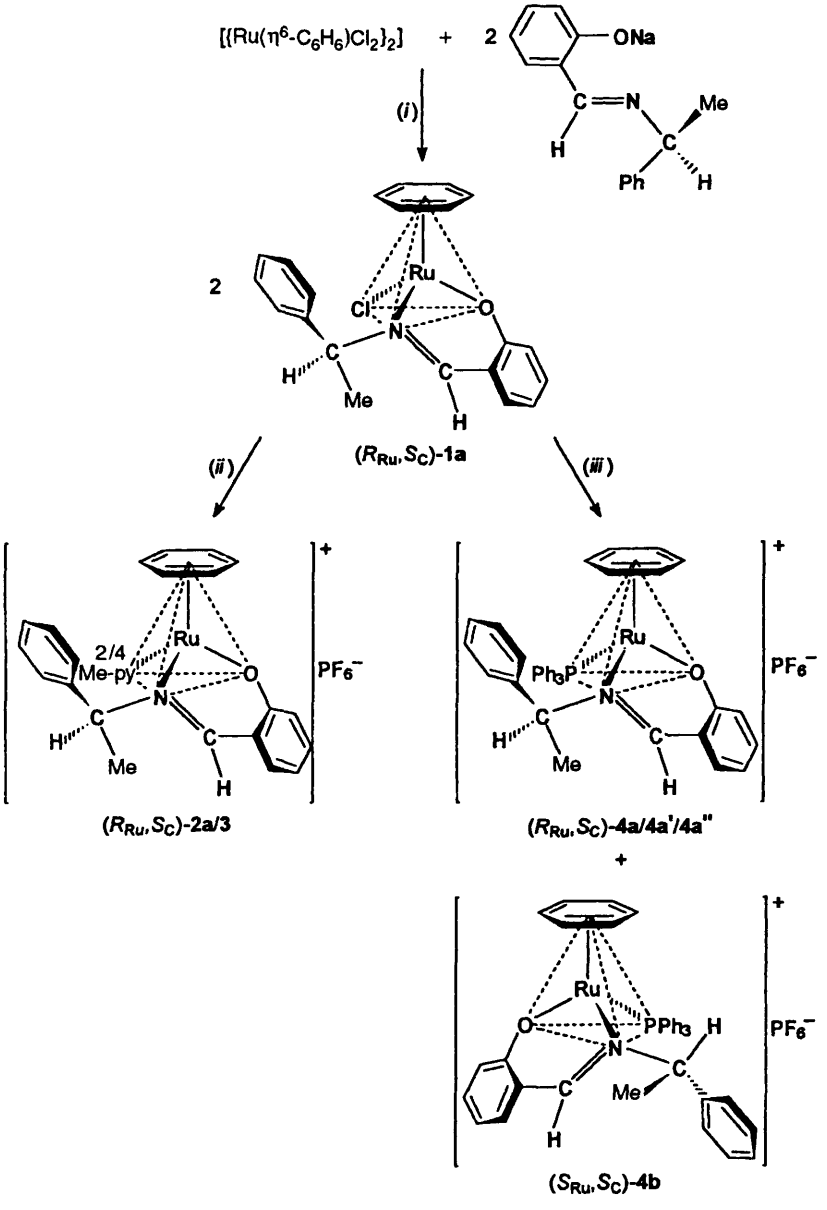

Scheme 1 (*i*) Na(L–L), CH_2Cl_2, 0–5 °C; (*ii*) acetone, −30 °C, (*a*) $AgPF_6$, (*b*) 4- or 2-Me-py; (*iii*) CH_2Cl_2, −30 to −35 °C, (*a*) PPh_3, (*b*) $AgPF_6$. Only the diastereomers obtained pure in the solid state are shown

crystals have a uniform shape, as confirmed with a microscope. Therefore, we conclude that the crystals **1a**, obtained in the crystallisation step after the synthesis, only contain molecules with (R_{Ru},S_C) configuration. On the other hand, the ^{1}H NMR spectra at room temperature and at −80 °C show the signals of both diastereomers **1a** and **1b** in a ratio of 86:14, indicating a rapid change of the ruthenium configuration in solution, even at −80 °C. Thus, the isolation of diastereomerically pure **1a** by crystallisation implies an asymmetric transformation of the second kind.[15] In contrast, the corresponding η^6-*p*-cymene complexes were erroneously reported to be configurationally stable up to 70 °C in benzene.[5b] Moreover, the configurational instability of the ruthenium configuration in (η^6-arene)-ruthenium chloro complexes with chiral amino acid anions as chelating ligands ascribed to the dissociation of the chloride ligand and the formation of solvate complexes was already known[16a,17] when refs. 5(*a*)–5(*c*) were published.

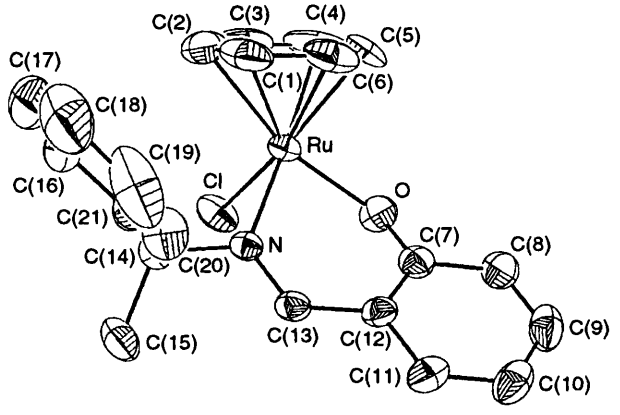

Fig. 1 An ORTEP view of the crystal structure of diastereomer **1a** with atom numbering. Thermal ellipsoids represent 40% probability contours. Hydrogen atoms have been omitted for clarity

The thermodynamically more stable diastereomer in solution, which is the major isomer showing the high-field ^{1}H NMR signal for the η^6-benzene ligand, is assigned to complex **1a** with (R_{Ru},S_C) configuration (Scheme 1). This assignment is based on the conformational analysis given below.

The shape of complex **1a** is determined by the orientation of the 1-phenylethyl group with respect to the [Ru(η^6-C_6H_6)(L–L)-Cl] moiety [rotation about the bond C(14)–N]. In the crystal structure, the hydrogen atom at C(74) is oriented towards the chloride ligand at a distance of 2.82 Å, smaller than the sum of the van der Waals radii of H and Cl.[18] Another conformation-determining effect is the attractive interaction caused by the face-on orientation of the phenyl ring relative to the η^6-benzene ligand. In the thermodynamically more stable isomers of many other transition-metal half-sandwich complexes the phenyl substituents adopt a similar orientation relative to the π-bonded arene ligand in the solid state.[16,19] This conformation is assumed to be retained in solution.[19] The stabilising nature of this interaction is called the 'β-phenyl effect'[19] and π–π edge-to-face or T-shaped interaction.[20,21]

Synthesis and characterisation of complexes 2a/2b and 3

The chloride ligand in complex **1** was abstracted in a slightly different manner from that published (Scheme 1).[5] Crystalline **1a** was suspended in acetone and $AgPF_6$ was added in an equimolar quantity after cooling the solution to −30 °C. This resulted in the formation of a red solution and a precipitate of AgCl. On addition of 4-methylpyridine or 2-methylpyridine at −30 °C there was a change in colour to yellow-orange. Evaporation of the solvent and recrystallisation from acetone–

Table 1 Summary of crystal data, data collection and structure refinement[a] for complexes **1a**, **2a** and **4a**″[b]

	1a	**2a**	**4a**″
Elemental formula	$C_{21}H_{20}ClNORu$	$C_{27}H_{27}F_6N_2OPRu$	$C_{39}H_{35}F_6NOP_2Ru{\cdot}CH_2Cl_2$
M	438.92	641.56	895.65
Crystal system	Rhombic	Monoclinic	Triclinic
Space group	$P2_12_12_1$ (no. 19)	$P2_1$ (no. 4)	*P*1 (no. 1)
a/Å	9.347(3)	10.117(3)	9.799(2)
b/Å	10.305(3)	10.686(2)	10.379(4)
c/Å	19.40(2)	12.610(3)	10.831(4)
α/°			117.77(2)
β/°			98.36(2)
γ/°			92.05(2)
U/Å^3	1868.6	1355.5	957.6
Z	4	2	1
D_c/g cm^3	1.56	1.57	1.55
F(000)	888	648	454
μ/mm^{-1}	0.97	0.69	0.69
Crystal colour, shape	Red-brown, long plates	Red-orange plates	Dark red prisms
Crystal size/mm	0.05 × 0.25 × 0.90	0.15 × 0.5 × 0.60	0.25 × 0.45 × 0.90
hkl Ranges	0–14, 0–15, 0–28	0–14, −15 to 15, −17[c] to 17	0–14, −15 to 15, −15 to 15
2θ Range/°	3.0–60	3.0–55.5	3.0–57.5
Total unique reflections	3103	6389	4993
No. observed reflections ($I > 2.5\sigma_I$)	2404	5613	4742
Minimum, maximum transmission factors	0.89, 1.00	0.84, 1.00	0.90, 1.00
No. reflections, 2θ range/° for empirical absorption correction	8, 7.9–45.5	7, 8.0–45.0	7, 4.0–41.0
No. of least-squares parameters	227	343	476
Largest shift/e.s.d. in final cycle	0.02	0.88	0.02[d]
$\Delta\rho_{min}$, $\Delta\rho_{max}$/e Å^{-3}	−0.51, 0.50	−0.59, 0.70	−0.52, 0.83
R[e]	0.037	0.034	0.048
R′[f]	0.034	0.034	0.046

[a] Syntex-Nicolet R3 diffractometer; Mo-Kα radiation (λ = 0.710 73 Å); 293 K; graphite-crystal monochromator; MicroVAX II computer. [b] (R_{Ru}, S_C)-[Ru(η^6-C_6H_6)(L–L)Cl] **1a**, (R_{Ru},S_C)-[Ru(η^6-C_6H_6)(L–L)(4Me-py)]PF_6 **2a**, (R_{Ru}, S_C, P_{PPh_3})-[Ru(η^6-C_6H_6)(L–L)(PPh_3)]$PF_6{\cdot}CH_2Cl_2$ **4a**″. [c] The crystal which is assigned to the monoclinic system was measured in the range $3.0 < 2\theta < 55.5°$ as belonging to the triclinic system in order to obtain the Friedel pairs for determination of the absolute configuration. [d] Shift/e.s.d.$_{max}$ = 0.2 for the PF_6 anion. [e] $R = \Sigma||F_o| - |F_c||/\Sigma|F_c|$. [f] $R' = \Sigma||F_o| - |F_c||w^{\frac{1}{2}}/\Sigma|F_o|w^{\frac{1}{2}}$, $w = 1/\sigma^2(F_o)$.

Table 2 Proton NMR data for complexes **1a/1b**, **2a (2b)**, **3**, **4a/4a′/4a″** and **4b**[a]

Complex	L–L	η^6-C_6H_6	L′[b]
1a/1b[c]	1.76/2.00 (3 H, d, $^3J_{HH}$ 7.0/6.9, CHCH_3) 5.78/5.68 (1 H, q, $^3J_{HH}$ 7.0/6.9, CHCH$_3$) 6.51/6.39 (1 H, ddd, $^3J_{HH}$ 7.9, 6.9, $^4J_{HH}$ 1.1, H^4 of sal)[d] 7.00/6.93 (1 H, d, $^3J_{HH}$ 8.5, H^6 of sal) 7.03/6.78 (1 H, dd, $^3J_{HH}$ 7.9, $^4J_{HH}$ 1.8, H^3 of sal) 7.23/7.16 (1 H, ddd, $^3J_{HH}$ 8.5, 6.9, $^4J_{HH}$ 1.8, H^5 of sal) 7.30–7.67 (5 H, m, Ph of sal) 7.99 (1 H, s, N=CH)	5.31/5.45	
2a (2b)[e]	1.86 (3 H, d, $^3J_{HH}$ 6.9, CHCH_3) 6.54 (6.61) [1 H, ddd, $^3J_{HH}$ 7.9 (8.0), 7.0 (7.0), $^4J_{HH}$ 1.1 (1.1), H^4 of sal] 6.65 (6.09) [1 H, q, $^3J_{HH}$ 6.9 (7.1), CHCH$_3$] 7.02 (1 H, d, $^3J_{HH}$ 8.6, H^6 of sal) 7.32 (1 H, dd, $^3J_{HH}$ 7.9, $^4J_{HH}$ 1.8, H^3 of sal) 7.38 (1 H, ddd, $^3J_{HH}$ 8.6, 7.0, $^4J_{HH}$ 1.8, H^5 of sal) 7.52–7.64 (6.99–7.16) (5 H, m, Ph) 8.57 (8.43) (1 H, s, N=CH)	5.78 (6.12)	2.45 (2.26) (3 H, s, CH$_3$) 7.51 (6.95) [2 H, dd, $^3J_{HH}$ 6.6 (6.7), $^4J_{HH}$ 0.6 (0.7), H^3/H^5] 8.70 (8.34) [2 H, d, $^3J_{HH}$ 6.6 (6.7), H^2/H^6]
3[f]	2.03 (3 H, d, $^3J_{HH}$ 6.6, CHCH_3) 6.38 (1 H, ddd, $^3J_{HH}$ 7.8, 7.0, $^4J_{HH}$ 1.1, H^4 of sal) 6.57 (1 H, q, $^3J_{HH}$ 6.6, CHCH$_3$) 6.88 (1 H, d, $^3J_{HH}$ 8.7, H^6 of sal) 7.00 (1 H, dd, $^3J_{HH}$ 7.8, $^4J_{HH}$ 1.8, H^3 of sal) 7.20 (1 H, ddd, $^3J_{HH}$ 8.7, 7.0, $^4J_{HH}$ 1.8, H^5 of sal) 7.40–7.53 (5 H, m, Ph of sal) 8.25 (1 H, s, N=CH)	5.76 (br s)	2.95 (3 H, br s, CH$_3$) 7.17–7.22 (1 H, br m, H^5) 7.34 (1 H, d, $^3J_{HH}$ 7.8, H^3) 7.72 (1 H, dd, $^3J_{HH}$ 7.8, $^4J_{HH}$ 1.5, H^4) 8.80 (1 H, br s, H^6)
4a/4a′/4a″[g]	0.73 (3 H, d, $^3J_{HH}$ 6.7, CHCH_3) 5.26 (1 H, q, $^3J_{HH}$ 6.7, CHCH$_3$) 6.70 (1 H, ddd, $^3J_{HH}$ 7.8, 7.0, $^4J_{HH}$ 1.0, H^4 of sal) 6.79 (1 H, d, $^3J_{HH}$ 8.6, H^6 of sal) 7.33 (1 H, ddd, $^3J_{HH}$ 8.6, 7.0, $^4J_{HH}$ 1.8, H^5 of sal) 7.52–7.71 (1 H, m, H^3 of sal)[h] 8.47 (1 H, d, $^3J_{HP}$ 1.7, N=CH) 7.52–7.71 (5 H, br m, Ph of sal)[h]	5.66 (d, $^3J_{HP}$ 0.3)	7.52–7.71 (15 H, br m, PPh$_3$)[h]
4b[g]	2.07 (3 H, br d, $^3J_{HH}$ 6.7, CHCH_3) 5.40 (1 H, q, $^3J_{HH}$ 6.7, CHCH$_3$) 6.30 (1 H, ddd, $^3J_{HH}$ 7.9, 7.0, $^4J_{HH}$ 1.1, H^4 of sal) 6.71 (1 H, d, $^3J_{HH}$ 8.6, H^6 of sal)[j] 7.01–7.11 (3 H, m, H^3 of sal + H$_m$ of Ph of sal) 7.08 (1 H, ddd, $^3J_{HH}$ 8.6, 7.0, $^4J_{HH}$ 1.8, H^5 of sal) 7.25 (1 H, m, H$_p$ of Ph of sal) 7.35 (2 H, $^3J_{HH}$ 7.4, H$_o$ of Ph of sal)[l] 7.62 (1 H, d, $^3J_{HP}$ 2.1, N=CH)	6.41[i]	6.00 (2 H, m, H$_o$) 6.51 (2 H, m, H$_m$) 6.90 (1 H, m, H$_p$) 7.63–7.71 (3 H, m) 7.72–7.76 (2 H, m) 7.81–7.85 (4 H, m) 7.98 (1 H, m, H$_p$)[k]

[a] [Ru(η^6-C_6H_6)(L–L)Cl] **1a/1b**, [Ru(η^6-C_6H_6)(L–L)(4Me-py)]PF_6 **2a/2b**, [Ru(η^6-C_6H_6)(L–L)(2Me-py)]PF_6 **3**, [Ru(η^6-C_6H_6)(L–L)(P-Ph$_3$)]PF_6·CH_2Cl_2 **4a″**. In all cases the isomers denoted **a** are the major diastereomers in solution. Data given as δ with J/Hz; s = singlet, d = doublet, q = quartet, m = multiplet, br = broad; $SiMe_4$ as standard. Assignments in the cases of complexes **2a** and **4a″** on the basis of proton–proton and –carbon two-dimensional correlation spectroscopy at −80 °C. [b] L′ = Cl **1**, 4-methylpyridine **2**, 2-methylpyridine **3** or PPh_3 **4**. [c] At 250 MHz, solvent $CDCl_3$, 21 °C. [d] sal = Aromatic ABCD system (salicyl part) of the chelating ligand. [e] At 400 MHz, solvent [$^2H_6$]acetone, −80 °C; the data in parentheses for diastereomer **2b** were determined from the room-temperature spectrum. [f] At 400 MHz, solvent [$^2H_6$]acetone, 21 °C, the signal for the 1-phenylethyl methyl substituent is hidden by the solvent signal. [g] At 400 MHz, solvent [$^2H_6$]acetone, −80 °C. [h] Signal is partially overlapped. [i] $^3J_{HP}$ not determined due to line broadening. [j] $^4J_{HH}$ not determined due to line broadening. [k] All the PPh_3 signals coalesce at *ca.* −20 °C on warming the sample. [l] AA′ part of an AA′BB′C system.

hexane (11:5 and 10:9, respectively) gave red-orange crystals of [Ru(η^6-C_6H_6)(L–L)(4Me-py)]PF_6 **2** and [Ru(η^6-C_6H_6)-(L–L)(2Me-py)]PF_6 **3**, respectively, suitable for X-ray analysis, in about 90% yield.

The ^{1}H NMR spectrum of complex **2** at room temperature in [$^2H_6$] acetone shows the presence of two diastereomers in a 67:33 ratio, assigned to **2a** and **2b** on the basis of the signals of the η^6-benzene ligands at δ 5.78 and 6.12 (Table 2). The high-field shift of the signal of the major diastereomer **2a** is again due to the 'β-phenyl effect'.[16,19] On dissolution of the crystals, used in the X-ray analysis (see below), in [$^2H_6$]acetone at −80 °C, ^{1}H NMR spectroscopy reveals the presence of only **2a**. Thus, there is an asymmetric transformation of the second kind[15] during crystallisation of **2a/2b** with regard to a change in the configuration at the ruthenium atom to give pure **2a**. The kinetics of this change was followed by integration of the η^6-benzene NMR signals. The reaction is first order in the concentration of **2a** and the half-life $\tau_{\frac{1}{2}}$ at −(35 ± 2) °C is 81.6 ± 0.4 min. As a consequence, the ruthenium configuration of the diastereomers **2a** and **2b** is unstable under the conditions of the synthesis and it is impossible to decide whether substitution of the chloride ligand occurs with retention or inversion of the ruthenium configuration. Therefore, the assignment of retention of stereochemistry upon chloride substitution in the η^6-*p*-cymene complexes is unjustified.[1,5,6] Mandal and Chakravarty incorrectly assumed configurational stability for the η^6-*p*-cymene complex containing the 4Me-py ligand.

The ^{1}H NMR spectrum of the 2-methylpyridine complex **3** in [$^2H_6$]acetone shows at room temperature and at low temperatures before and after recrystallisation only the signals of one diastereomer. The similarities of the chemical shifts compared to those of **2a**, in particular that of the η^6-benzene ligand (see Table 2), prompts us to suggest that the configuration of **3** is the same as in the thermodynamically more stable isomer (R_{Ru},S_C)-**2a**. Interestingly, the signals of all the hydrogens, which are influenced by a rotation of the 2-methylpyridine ligand about the ruthenium–nitrogen bond, are

Table 3 Positional parameters ($\times 10^4$) for the complexes **1a**, **2a** and **4a″** with their estimated standard deviations (e.s.d.s) in parentheses

Atom	*x*	*y*	*z*	Atom	*x*	*y*	*z*
Complex **1a**							
Ru	8 753(1)	52(1)	7 970(1)	C(10)	7 089(9)	−2 013(7)	5 417(3)
Cl	7 175(2)	1 890(1)	8 142(1)	C(11)	6 473(7)	−2 023(6)	6 062(3)
O	8 644(5)	431(4)	6 927(2)	C(12)	7 007(6)	−1 248(5)	6 604(3)
N	6 819(5)	−949(4)	7 846(2)	C(13)	6 323(6)	−1 348(5)	7 264(3)
C(1)	9 630(8)	−1 373(9)	8 677(5)	C(14)	5 920(6)	−1 116(6)	8 484(3)
C(2)	9 509(9)	−236(10)	9 027(4)	C(15)	4 302(6)	−967(7)	8 356(4)
C(3)	10 073(11)	840(10)	8 766(6)	C(16)	6 584(7)	−2 327(8)	9 538(3)
C(4)	10 833(9)	871(9)	8 163(6)	C(17)	6 921(10)	−3 478(9)	9 881(4)
C(5)	10 978(6)	−357(10)	7 798(4)	C(18)	6 936(11)	−4 619(9)	9 546(5)
C(6)	10 369(8)	−1 451(7)	8 069(5)	C(19)	6 597(10)	−4 688(7)	8 871(6)
C(7)	8 162(7)	−405(6)	6 477(3)	C(20)	6 240(8)	−3 556(6)	8 510(3)
C(8)	8 801(8)	−437(6)	5 806(3)	C(21)	6 266(7)	−2 377(5)	8 841(3)
C(9)	8 254(8)	−1 219(7)	5 299(3)				
Complex **2a**							
Ru	9 556(1)	10 000	8 332(1)	C(17)	5 667(6)	9 797(8)	4 384(5)
O	10 962(4)	8 619(4)	8 480(3)	C(18)	5 827(6)	8 538(7)	4 322(5)
N(1)	9 865(3)	10 147(6)	6 709(3)	C(19)	6 928(5)	7 956(6)	4 870(4)
C(1)	8 450(10)	8 858(10)	9 270(11)	C(20)	7 889(5)	8 684(5)	5 432(4)
C(2)	8 940(7)	9 800(18)	9 891(5)	C(21)	7 785(4)	9 937(7)	5 450(3)
C(3)	8 631(10)	11 032(13)	9 517(10)	N(2)	11 252(5)	11 202(5)	8 549(4)
C(4)	7 835(10)	11 144(6)	8 574(10)	C(22)	11 325(5)	12 259(4)	7 956(4)
C(5)	7 384(6)	10 103(12)	8 025(5)	C(23)	12 406(6)	13 046(5)	8 092(4)
C(6)	7 694(8)	8 970(10)	8 401(7)	C(24)	13 471(6)	12 770(6)	8 846(5)
C(7)	11 929(4)	8 472(4)	7 886(4)	C(25)	13 383(5)	11 713(6)	9 436(4)
C(8)	13 009(5)	7 681(5)	8 256(4)	C(26)	12 285(5)	10 944(5)	9 292(3)
C(9)	14 095(5)	7 561(6)	7 720(5)	C(27)	14 645(7)	13 694(8)	8 998(6)
C(10)	14 191(5)	8 190(6)	6 773(4)	P	11 870(1)	9 889(2)	2 634(1)
C(11)	13 161(5)	8 909(5)	6 356(4)	F(11)	10 711(6)	9 246(6)	3 119(5)
C(12)	12 017(4)	9 072(4)	6 890(3)	F(12)	13 108(5)	10 477(5)	2 214(5)
C(13)	10 932(4)	9 763(4)	6 351(3)	F(13)	10 971(6)	11 003(5)	2 251(5)
C(14)	8 858(5)	10 850(5)	5 971(3)	F(14)	12 792(5)	8 774(4)	3 021(4)
C(15)	9 479(6)	11 635(5)	5 135(5)	F(15)	11 481(6)	9 155(5)	1 571(3)
C(16)	6 635(5)	10 486(6)	4 927(5)	F(16)	12 257(5)	10 551(5)	3 722(3)
Complex **4a″**							
Ru	5 000	5 000	5 000	C(24)	10 613(9)	4 009(11)	7 971(12)
P(1)	4 849(2)	6 522(2)	3 899(2)	C(25)	10 405(9)	3 569(10)	6 519(10)
N	6 659(6)	6 450(7)	6 547(6)	C(26)	9 575(8)	4 313(9)	5 996(9)
O	3 678(5)	6 338(6)	6 161(5)	C(27)	8 891(7)	5 454(8)	6 875(7)
C(1)	6 504(6)	7 441(7)	7 784(7)	C(28)	3 909(7)	7 085(7)	7 545(7)
C(2)	8 101(6)	6 326(8)	6 260(7)	C(29)	2 787(7)	7 330(8)	8 261(8)
C(3)	8 986(9)	7 787(10)	6 798(11)	C(30)	2 935(9)	8 234(8)	9 706(8)
C(4)	6 921(8)	8 771(9)	4 343(9)	C(31)	4 257(10)	8 894(9)	10 494(8)
C(5)	7 690(9)	10 089(10)	5 156(11)	C(32)	5 368(8)	8 647(8)	9 852(7)
C(6)	7 474(10)	10 990(10)	6 486(11)	C(33)	5 255(7)	7 723(7)	8 366(7)
C(7)	6 429(9)	10 602(9)	7 037(9)	C(34)	4 363(14)	3 212(10)	5 472(10)
C(8)	5 644(8)	9 273(8)	6 208(8)	C(35)	3 377(9)	3 192(9)	4 377(11)
C(9)	5 889(7)	8 316(8)	4 875(7)	C(36)	3 753(9)	3 058(9)	3 157(9)
C(10)	4 547(9)	5 751(8)	1 007(7)	C(37)	5 185(9)	2 993(8)	3 030(8)
C(11)	5 029(11)	5 210(10)	−276(8)	C(38)	6 147(9)	3 043(9)	4 133(10)
C(12)	6 301(10)	4 701(10)	−393(9)	C(39)	5 767(12)	3 165(9)	5 325(10)
C(13)	7 094(9)	4 634(10)	751(9)	P(2)	−592(2)	1 403(3)	1 502(2)
C(14)	6 602(8)	5 159(9)	2 010(8)	F(11)	−1 947(11)	1 548(18)	1 792(16)
C(15)	5 365(7)	5 737(7)	2 175(7)	F(12)	−51(17)	1 429(12)	2 888(9)
C(16)	1 941(7)	6 170(10)	3 464(8)	F(13)	851(10)	1 095(18)	1 228(13)
C(17)	626(9)	6 516(12)	3 131(10)	F(14)	−1 028(22)	1 395(18)	174(11)
C(18)	463(9)	7 689(13)	2 909(10)	F(15)	−474(23)	3 009(10)	2 323(12)
C(19)	1 654(11)	8 568(12)	3 056(10)	F(16)	−810(14)	−237(9)	746(13)
C(20)	2 956(9)	8 240(10)	3 392(9)	C(40)	1 992(13)	740(12)	8 400(11)
C(21)	3 106(7)	7 011(8)	3 579(7)	Cl(1)	1 813(4)	136(4)	6 617(3)
C(22)	9 079(8)	5 817(9)	8 305(8)	Cl(2)	3 390(4)	2 062(5)	9 329(4)
C(23)	9 944(10)	5 093(10)	8 825(9)				

broadened significantly at room temperature. These are the signals for pyridine H^6 (δ 8.80), CH of the 1-phenylethyl group (δ 6.57), η^6-C_6H_6 (δ 5.76) and CH_3 of the pyridine ligand (δ 2.95). The reason for this line broadening is the hindrance to rotation. On cooling the sample to −80 °C, all the signals split reversibly into signals for two atropisomers in a ratio of 54:46. By measuring the line broadening of the well separated signals of the imine protons above and below the coalescence temperature the free energy of activation for the rotational process was determined[22] to be $\Delta G^{\ddagger} = 44.5 \pm 0.5$ kJ mol^{-1}.

The conclusion from these results is that in the 2-methylpyridine series only the diastereomer with (R_{Ru},S_C) configuration **3a** is stable. In the hypothetical diastereomer (S_{Ru},S_C)-**3b**, a conformation of the 1-phenylethyl group with a face-on orientation of the phenyl substituent with respect to the

Table 4 Selected bond lengths (Å) and angles (°) for complexes **1a**, **2a** and **4a″** with e.s.d.s in parentheses

Complex **1a**			
Ru–O	2.062(4)	Cl–Ru–O	87.6(1)
Ru–N	2.095(5)	Cl–Ru–N	82.9(1)
Ru–Cl	2.424(3)	O–Ru–N	86.5(2)
Ru–C(1)	2.171(9)	Ru–O–C(7)	123.2(4)
Ru–C(2)	2.189(9)	Ru–N–C(13)	124.6(4)
Ru–C(3)	2.138(11)	O–C(7)–C(12)	123.6(5)
Ru–C(4)	2.153(9)	C(7)–C(12)–C(13)	122.8(5)
Ru–C(5)	2.148(7)	N–C(13)–C(12)	126.8(5)
Ru–C(6)	2.172(7)	C(1)–Ru–C(2)	36.3(4)
O–C(7)	1.307(7)	C(1)–Ru–C(6)	36.8(3)
N–C(13)	1.287(7)	C(2)–Ru–C(3)	35.7(4)
N–C(14)	1.505(7)	C(3)–Ru–C(4)	37.2(4)
		C(4)–Ru–C(5)	39.6(4)
		C(5)–Ru–C(6)	36.9(3)
Complex **2a**			
Ru–O	2.044(4)	O–Ru–N(2)	83.2(2)
Ru–N(1)	2.109(3)	N(1)–Ru–N(2)	83.1(2)
Ru–N(2)	2.138(5)	O–Ru–N(1)	88.2(2)
Ru–C(1)	2.103(12)	Ru–O–C(7)	126.3(3)
Ru–C(2)	2.135(7)	Ru–N(1)–C(13)	122.4(3)
Ru–C(3)	2.151(13)	O–C(7)–C(12)	125.1(4)
Ru–C(4)	2.175(9)	C(7)–C(12)–C(13)	122.3(4)
Ru–C(5)	2.193(6)	N(1)–C(13)–C(12)	129.0(4)
Ru–C(6)	2.192(9)	C(1)–Ru–C(2)	36.8(6)
O–C(7)	1.303(6)	C(1)–Ru–C(6)	34.4(4)
N(1)–C(13)	1.281(6)	C(2)–Ru–C(3)	38.8(6)
N(1)–C(14)	1.505(6)	C(3)–Ru–C(4)	36.9(4)
		C(4)–Ru–C(5)	36.4(4)
		C(5)–Ru–C(6)	35.2(4)
Complex **4a″**			
Ru–O	2.040(5)	O–Ru–P(1)	82.7(2)
Ru–N	2.097(5)	N–Ru–P(1)	90.3(2)
Ru–P(1)	2.379(3)	O–Ru–N	88.2(2)
Ru–C(34)	2.234(12)	Ru–O–C(28)	124.5(4)
Ru–C(35)	2.191(9)	Ru–N–C(1)	123.0(5)
Ru–C(36)	2.215(7)	O–C(28)–C(33)	122.7(6)
Ru–C(37)	2.218(7)	C(1)–C(33)–C(28)	123.5(5)
Ru–C(38)	2.228(8)	N–C(1)–C(33)	128.2(5)
Ru–C(39)	2.229(11)	C(34)–Ru–C(35)	37.1(4)
O–C(28)	1.306(8)	C(34)–Ru–C(39)	36.8(5)
N–C(1)	1.290(8)	C(35)–Ru–C(36)	36.2(4)
N–C(2)	1.487(9)	C(36)–Ru–C(37)	37.6(3)
		C(37)–Ru–C(38)	36.4(3)
		C(38)–Ru–C(39)	35.1(4)

η^6-benzene ligand would imply an orientation of the methyl substituent towards the pyridine ligand, increasing the steric hindrance.

Crystal structure of diastereomer 2a

An ORTEP view of the cation of diastereomer **2a** is shown in Fig. 2. Atomic coordinates and selected bond distances and angles are given in Tables 3 and 4. The crystal structure confirms the (S_C) configuration of the stereogenic carbon centre. The configuration of the ruthenium centre was specified using the priority sequence η^6-C_6H_6 > O (L–L) > N (L–L) > N (4Me-py) and is (R_{Ru}).[14] There is a double change in the priority sequence of the ligands in **2a** compared to that in **1a**. Thus, the configurational symbols are the same. In the η^6-benzene complex **2a** the ruthenium atom has the same configuration as that in the analogous η^6-*p*-cymene complex, the crystal structure of which has recently been published.[1] As in the latter crystal structure, the bond between the pyridine N(2) and Ru in **2a** is 0.03 Å longer than that between the imine nitrogen N(1) and Ru.[1] The average of the bond lengths Ru–C(1–6) is about 0.03 Å shorter than that in the η^6-*p*-cymene complex.[1] This is presumably due to the lower Lewis basicity of the η^6-*p*-benzene ligand with respect to the dialkyl substitution of the η^6-*p*-cymene ligand. Steric reasons may also be responsible for this effect.[23] The phenyl substituent of the

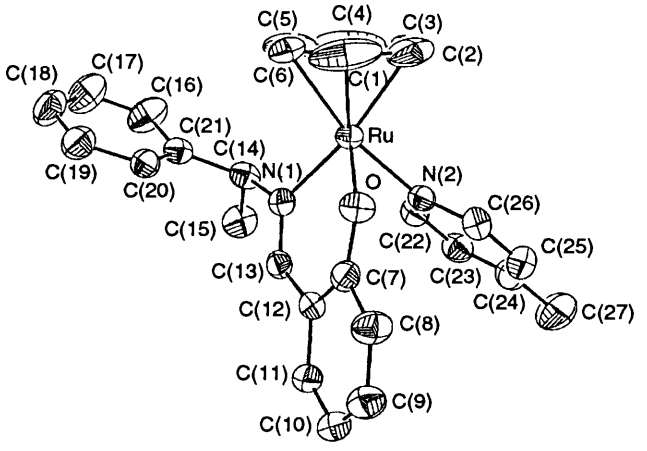

Fig. 2 An ORTEP view of the molecular structure of the cation of diastereomer **2a** with atom numbering. Hydrogen atoms and the PF_6 anion have been omitted for clarity. Thermal ellipsoids are drawn at the 40% probability level

phenylethyl group is oriented in the favoured face-on manner with respect to the η^6-benzene ligand. This 'β-phenyl effect'[16,19] is also seen in the thermodynamically more stable η^6-*p*-cymene diastereomer.[1]

Synthesis and characterisation of the diastereomeric complexes 4a/4a′, 4b and 4a″

The synthesis, properties and crystal structures of (R_{Ru},S_C,M_{PPh_3}) and (R_{Ru},S_C,P_{PPh_3})-[Ru(η^6-C_6H_6)(L–L)(PPh_3)]PF_6, **4a** and **4a′** with different triphenylphosphane helicities have been published.[7] The (R_{Ru},S_C) diastereomer **4a**/**4a′** is the thermodynamically more stable and the (S_{Ru},S_C) diastereomer **4b** the less stable of the mixture. The equilibrium ratio in $CDCl_3$ at room temperature is 95:5.[7] In this paper we describe a preparative route to **4b** (Scheme 1). The chloride ligand in **1** was abstracted with $AgPF_6$ in CH_2Cl_2 at −35 °C. After addition of triphenylphosphane, the insoluble AgCl was filtered off at about −55 °C. The solution was concentrated while cold and the diastereomer mixture was precipitated by addition of cold (about −50 °C) light petroleum in small portions. The ^{1}H NMR spectrum measured at −50 °C of a sample of the mixture dissolved at −80 °C in [$^2H_6$]acetone showed the presence of the two diastereomers, especially the intense signals for the η^6-benzene ligand at δ 5.66 for **4a**/**4a′** and 6.41 for **4b**. The ratio of diastereomers **4a**/**4a′**:**4b** = 1:1 measured at −50 °C is far from the equilibrium ratio. Thus, the two diastereomers **4a**/**4a′** and **4b** are formed under kinetic reaction control.

The diastereomers **4a**/**4a′** and **4b** were separated on the basis of their different solubilities in $CHCl_3$. The mixture was stirred with $CHCl_3$ at −60 °C and the suspension was filtered while cold. From the cold filtrate it is possible to isolate the two crystalline modifications **4a** and **4a′** of the thermodynamically more stable diastereomer as described.[6,7] The residue after filtration was dissolved in CH_2Cl_2 at −60 °C and precipitated by slow addition of light petroleum at −35 °C, giving the thermodynamically less stable diastereomer **4b** with the low-field ^{1}H NMR signal for the η^6-benzene ligand. A sample of the orange product was dissolved in [$^2H_6$]acetone at −80 °C. The ^{1}H NMR spectrum at −80 °C showed more than 99% diastereomer purity for (S_{Ru},S_C)-**4b** (Table 2).

On cooling solutions of the two modifications **4a** and **4a′** in [$^2H_6$]acetone or CD_2Cl_2 to −80 °C the ^{1}H and ^{13}C-{^{1}H} NMR signals of the triphenylphosphane ligand broadened without any splitting in the range δ 7.52–7.64 (Tables 2 and 5).[7] In contrast, those of the triphenylphosphane ligand of diastereomer **4b** split into well resolved signals for the *o*-, *m*-, *p*-protons/carbons and, in case of the ^{13}C-{^{1}H} NMR spectra, for the *ipso*-carbons (Tables 2 and 5). The splitting pattern

Table 5 ^{13}C-{^1H} NMR data for the diastereomeric complexes **4a**/**4a′**/**4a″** and **4b**[a]

Complex	L–L	η^6-C_6H_6	PPh_3
4a/**4a′**/**4a″**[b]	25.3 ($CHCH_3$), 77.9 (d, $^3J_{CP}$ 2.5, $CHCH_3$), 116.6 (C^4 of sal), 122.7 (C^6 of sal), 123.0 (C^2 of sal), 126.0 (C_o of Ph of sal), 129.1 (C_p of Ph of sal), 130.2 (C_m of Ph of sal), 135.1/136.4 (C^3/C^5 of sal), 142.8 (C^1 of sal), 166.0 (C_{ipso} of Ph), 166.4 (N=CH)	90.4 (91.1) (d, $^3J_{CP}$ 2.9)[c]	129.3 (d, $^3J_{CP}$ 10.2, C_m), 130.7 (d, $^1J_{CP}$ 47.5, C_{ipso}), 131.9 (d, $^4J_{CP}$ 2.4, C_p), 134.2 (d, $^2J_{CP}$ 9.9, C_o)[d]
4b[e]	24.3 ($CHCH_3$), 79.4 ($CHCH_3$), 114.5 (br s, C^4 of sal), 121.0 (C^6 of sal), 123.1 (C^2 of sal), 128.6 (C_o of Ph), 128.7 (C_p of Ph), 128.8 (C_m of Ph), 135.0/135.9 (C^3/C^5 of sal), 140.7 (C^1 of sal), 162.2 (C_{ipso} of Ph), 166.5 (N=CH)	91.5[f]	125.9 (d, $^1J_{CP}$ 46.9, C_{ipso}), 127.6 (br s, C_m), 129.3 (br d, $^3J_{CP}$ 9.6, C_m), 130.0 (br s, C_m), 130.1 (s, C_p), 130.5 (d, $^1J_{CP}$ 45.5, C_{ipso}), 131.9 (br s, C_p), 132.9 (br s, C_p), 133.8 (d, $^2J_{CP}$ 9.0, C_o), 134.1 (d, $^2J_{CP}$ 9.0, C_o), 135.0 (d, $^1J_{CP}$ 46.0, C_{ipso}), 136.0 (m, C_o)[g]

[a] (R_{Ru},S_C,M_{PPh_3})- and (R_{Ru},S_C,P_{PPh_3})-[Ru(η^6-C_6H_6)(L–L)(PPh_3)]PF_6 **4a** and **4a′**, (R_{Ru},S_C,P_{PPh_3})-[Ru(η^6-C_6H_6)(L–L)(PPh_3)]PF_6·CH_2Cl_2 **4a″** and (S_{Ru},S_C)-[Ru(η^6-C_6H_6)(L–L)(PPh_3)]PF_6 **4b**; δ with J in Hz. [b] At 100.6 MHz, solvent CD_2Cl_2, standard $SiMe_4$, 21 °C. [c] δ in parentheses for diastereomer **4b**. [d] All the PPh_3 signals show only strong line broadening on cooling the sample to −90 °C. [e] At 100.6 MHz, solvent [$^2H_6$]acetone, standard $SiMe_4$, −80 °C, signal assignment on the basis of proton–carbon and –proton two-dimensional correlation spectroscopy. [f] $^3J_{CP}$ not determined due to line broadening. [g] All the PPh_3 signals show coalescence on warming the sample above −35 °C.

indicates a freezing of the rotation of the triphenylphosphane ligand about the ruthenium–phosphorus bond.[24] The ^1H NMR signals for one of the triphenylphosphane phenyls show a strong high-field shift (a multiplet at δ 6.00 for two *o*-protons, a multiplet at δ 6.51 for two *m*-protons and a multiplet at δ 6.90 for the *p*-proton). The linewidth of the ^{31}P-{^1H} NMR signal was not affected by cooling. On warming the sample to −20 °C there was not only broadening and coalescence of all the signals of the triphenylphosphane ligand of **4b** but also the ^1H NMR signal of the η^6-benzene ligand of the thermodynamically more stable diastereomer **4a**/**4a′** appeared at δ 5.66. On the other hand there was no coalescence of the signals of the phenyl substituent of the 1-phenylethyl group in the measured temperature range. Thus, by warming solutions of **4b** from −80 °C the triphenylphosphane ligand begins to rotate and due to increasingly unfavourable interactions between the rotating phosphane ligand and the other ligands the metal configuration becomes unstable. The half-life $\tau_{\frac{1}{2}}$ = 24.9 ± 0.01 min of the epimerisation **4a**/**4a′** ⇌ **4b** at −(1.0 ± 0.3) °C in [$^2H_6$]-acetone was measured by following the time-dependent ratio of the η^6-benzene signals of **4a**/**4a′** and **4b**, either **4a**/**4a′** or **4b** being the starting material (equilibrium ratio **4a**:**4b** = 93.4:6.6). This epimerisation in $CDCl_3$ (half-life $\tau_{\frac{1}{2}}$ = 25.7 ± 0.03 min, 12.0 ± 0.3 °C) has previously been addressed.[7] The results of the kinetic measurements and the implications with regard to the mechanism of the change in ruthenium configuration will be reported in a subsequent paper. Erroneously, Mandal and Chakravarty[5a,b] assumed their η^6-*p*-cymene complexes containing the triphenylphosphane ligand to be configurationally stable. Thus, they described the isolation of the pure (R_{Ru},S_C) diastereomer by column chromatography on SiO_2 at room temperature and subsequent crystallisation.

For comparison, an optically inactive complex [Ru(η^6-C_6H_6)(L–L)(PPh_3)]PF_6 (L–L = *N*-*tert*-butylsalicylideneaminate) was prepared by a similar synthetic route to that for complexes **4**. In contrast to the latter, this complex is unstable at room temperature and the ^1H and ^{13}C-{^1H} NMR spectra of a freshly prepared sample show only broad signals for the triphenylphosphane nuclei,* indicating that rotation of the phosphane ligand about the ruthenium–phosphorus bond is seriously hindered.

Crystal structure of diastereomer 4a″

Many attempts to obtain single crystals of complex **4b** of X-ray quality by crystallisation at temperatures below −20 °C have failed. In one experiment a sample of microcrystalline **4b** was dissolved in CH_2Cl_2–light petroleum (3:2) at −35 °C. The solution was kept in a cooling bath at −20 °C. During 62 h the bath and the solution warmed up to 3 °C and red-orange prisms of **4a″** formed in 12% yield. An ORTEP view of the cation of **4a″** is shown in Fig. 3. Positional parameters and bond lengths and angles are given in Tables 3 and 4. The crystal structure reveals the (R_{Ru},S_C,P_{PPh_3}) configuration of the cation of **4a″** and the presence of one equivalent of CH_2Cl_2 in the unit cell. Therefore, a configurational change from (S_{Ru},S_C) in **4b** to (R_{Ru},S_C) in **4a″** must have occurred during crystallisation. The dihedral angles of **4a″**, which define the triphenylphosphane helicity, are within a few degrees identical to those of modification **4a′**, the structure of which was published recently.[7] As in the structures of **4a** and **4a′**[7] and of **1a** and **2a**, the phenyl substituent in **4a″** is oriented face-on with respect to the η^6-benzene ligand. In contrast to the structures of **4a** and **4a′**,[7] in **4a″** there are no non-bonding distances shorter than the van der Waals radii.[18]

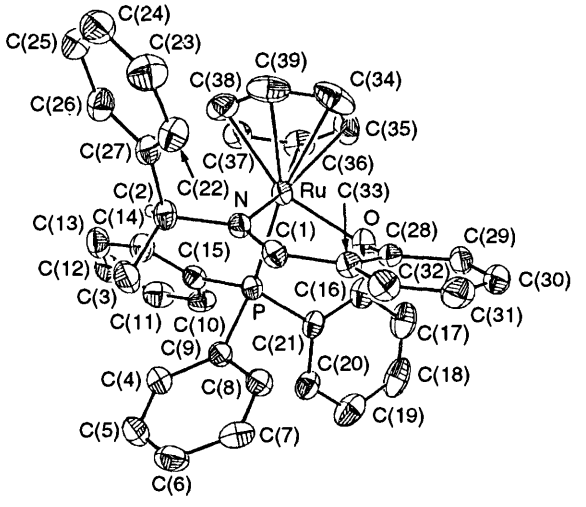

Fig. 3 An ORTEP view of the molecular structure of the cation of diastereomer **4a″** with atom numbering. Thermal ellipsoids represent 40% probability contours. Hydrogen atoms, the PF_6 anion and the CH_2Cl_2 molecule have been omitted for clarity

Chiroptical properties of the diastereomer mixture of complexes 1 and 2 and diastereomers 3, 4a″ and 4b

The optical rotations were measured at room temperature for the diastereomer mixtures **1a**:**1b** = 86:14 in the solvent CH_2Cl_2 and **2a**:**2b** = 76:24 in acetone. Those of the diastereomers **4a**/**4a′** and **4b** were determined in CH_2Cl_2 at −18 and −35 °C, at which the epimerisation reaction is slow.

* Chemical shift ranges for PPh_3 (CD_2Cl_2, 21 °C, solvent signal as reference): ^1H, δ 7.30–7.80; ^{13}C-{^1H}, δ 128–130, 131–133, and 133–135.

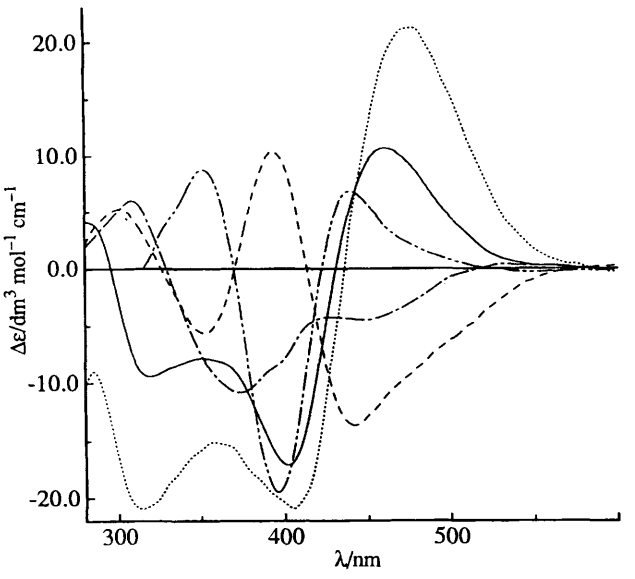

Fig. 4 The CD spectra of complexes **1a/1b**, **2a/2b**, **3**, **4a/4a′** and **4b**. c = (2.34–9.57) × 10^{-4} mol dm^{-3}, CH_2Cl_2: · · ·, **1** (22 °C); —, **2** (22 °C); · · ·, **3** (22 °C); – – –, **4a/4a′/4a″** (−21 °C); – · · –, **4b** (−35 °C)

Although the (R_{Ru},S_C,M_{PPh_3}) and (R_{Ru},S_C,P_{PPh_3}) diastereomers **4a** and **4a′/4a″**, respectively, and (S_{Ru},S_C) **4b** have opposite ruthenium configurations, they all have negative optical rotations at the sodium D line ($[\alpha]_{589}{}^{18}$ = −1076 for **4a/4a′** and $[\alpha]_{589}{}^{35}$ = −92 for **4b**; c = 0.08, CH_2Cl_2). This is exceptional, because usually there is a correlation between the metal configuration and the sign of optical rotation, *e.g.* in the series [Re(η^5-C_5H_5)(NO)(PPh_3)L] (L = monodentate ligand).[25]

In Fig. 4 the CD spectra of the diastereomer mixtures **1a/1b** and **2a/2b**, of complex **3** and of the diastereomers (R_{Ru},S_C) **4a/4a′** and (S_{Ru},S_C) **4b** are shown. The CD spectra of the diastereomers **4a/4a′** and **4b** were measured at −21 and −35 °C. The spectra of the η^6-benzene complexes in Fig. 4 are similar to those of the published η^6-*p*-cymene complexes.[5] Obviously, only the CD spectra of the diastereomer mixture **2a/2b**, of complex **3** and of diastereomer **4b** are similar to each other, whereas the spectrum of **4a/4a′** is close to being that of the mirror image. The CD spectrum of the chloro complexes **1a/1b**, however, differs appreciably from the other spectra and no safe conclusions can be drawn from comparisons with them.

To complex **2a**, the major diastereomer in the equilibrium **2a** ⇌ **2b**, and to the pure diastereomer **3** the same (R_{Ru}) configuration was assigned. In accord, their CD spectra are similar (Fig. 4). This is to be expected due to the similarity of the two ligands 4- and 2-methylpyridine. The intensity differences in the spectra of **2a/2b** and **3** are understandable because **3** is diastereomerically pure whereas the spectrum of **2a/2b** is a superposition of the spectra of **2a** and **2b**. In organotransition-metal complexes with stereogenic metal centres the CD spectra are primarily influenced by the metal chromophore.[2b,26] Therefore, diastereomers such as **2a** and **2b**, differing only in the metal configuration, to a first approximation have mirror-image CD spectra. As a consequence, the main contribution of the minor diastereomer **2b** to the CD spectrum of the major diastereomer **2a** is a reduction of the intensity.

Complex **2a**, the major diastereomer in the **2a/2b** mixture, and the diastereomers **4a/4a′/4a″** have the same ruthenium configuration, as demonstrated by X-ray analyses (Figs. 2 and 3; ref. 7). Their CD spectra, however, are approximately mirror images of each other. Thus, it must be concluded that in the complexes [Ru(η^6-C_6H_6)(L–L)L′]PF_6 the ligands L′ = 4-methylpyridine and triphenylphosphane make extremely different contributions to the circular dichroism.

Mandal and Chakravarty[5a,b] determined the configuration of the (η^6-*p*-cymene)ruthenium complex containing the triphenylphosphane ligand by X-ray analyses. Two cations with different triphenylphosphane helicities and two different anions but the same ruthenium configurations as in the diastereomers **4a/4a′/4a″** with the η^6-benzene ligand were found. As the CD spectrum of the complex with the triphenylphosphane ligand was nearly the mirror image of the spectra of the diastereomer mixtures of the chloro complex and the cationic 4-methylpyridine complex, opposite configurations were assigned to them.[5] This conclusion is wrong for the 4-methylpyridine complex and speculative for the chloro complex (see above). In addition, the configurational lability of all the compounds under discussion precludes the assignment of retention or inversion of stereochemistry to the substitution reactions.[1]

Conclusions

In (η^6-benzene)ruthenium complexes [Ru(η^6-C_6H_6)(L–L)L′] and [Ru(η^6-C_6H_6)(L–L)L′]PF_6 with L–L = (*S*)-*N*-(1-phenylethyl)salicylideneaminate and L′ = chloride, 4- and 2-methylpyridine, or triphenylphosphane there is a correlation between the conformation of the 1-phenylethyl group ('β-phenyl effect'[16,19]) and the configuration of the ruthenium atom (two diastereomers possible). In the thermodynamically more stable diastereomers the C–H bond of the 1-phenylethyl substituent is oriented towards the unidentate ligand to minimise steric hindrance. At the same time the phenyl substituent of the 1-phenylethyl group takes up a face-on orientation relative to the η^6-benzene ligand ('β-phenyl effect'[16,19]).

Acknowledgements

We thank the Deutsche Forschungsgemeinschaft, the Fonds der Chemischen Industrie and BASF AG, Ludwigshafen, for support of this work.

References

1 Part 106, H. Brunner, R. Oeschey and B. Nuber, *Inorg. Chem.*, 1995, **34**, 3349.
2 (*a*) H. Brunner, *Acc. Chem. Res.*, 1979, **12**, 250; (*b*) H. Brunner, *Top. Curr. Chem.*, 1980, **56**, 67; (*c*) H. Brunner, *Adv. Organomet. Chem.*, 1980, **18**, 151; (*d*) K. Blackburn, S. G. Davies and M. Whittaker, *Chemical Bonds–Better Ways to Make Them and to Break Them*, ed. I. Bernal, Elsevier, New York, 1989, pp. 141–223; (*e*) G. A. Stark, M. A. Dewey, G. B. Richter-Addo, D. A. Knight, A. M. Arif and J. A. Gladysz, *Stereoselective Reactions of Metal-Activated Molecules*, eds. H. Werner and J. Sundermeyer, Vieweg, Stuttgart, 1995, pp. 51–72.
3 G. Consiglio and F. Morandini, *Chem. Rev.*, 1987, **87**, 761; M. O. Albers, D. J. Robinson and E. Singleton, *Coord. Chem. Rev.*, 1987, **79**, 1.
4 F. Hapiot, F. Agbossou and A. Mortreux, *Tetrahedron: Asymmetry*, 1994, **5**, 515; P. Krasik and H. Alper, *Tetrahedron*, 1994, **50**, 4347; W.-Chung Chan, C.-P. Lau, L. Cheng and Y.-S. Leung, *J. Organomet. Chem.*, 1994, **464**, 103; B. Seiller, C. Bruneau and P. H. Dixneuf, *J. Chem. Soc., Chem. Commun.*, 1994, 493; K. T. Wan and M. E. Davies, *Nature (London)*, 1994, **370**, 449.
5 S. K. Mandal and A. R. Chakravarty, (*a*) *J. Organomet. Chem.*, 1991, **417**, C59; (*b*) *J. Chem. Soc., Dalton Trans.*, 1992, 1627; (*c*) *Inorg. Chem.*, 1993, **32**, 3851.
6 R. Oeschey, Ph.D. Thesis, University of Regensburg, 1995.
7 H. Brunner, R. Oeschey and B. Nuber, *Angew. Chem.*, 1994, **106**, 941; *Angew. Chem., Int. Ed. Engl.*, 1994, **33**, 866.
8 G. Winkhaus and H. Singer, *J. Organomet. Chem.*, 1967, **7**, 487; R. A. Zelonka and M. C. Baird, *Can. J. Chem.*, 1972, **50**, 3063; M. A. Bennett and A. K. Smith, *J. Chem. Soc., Dalton Trans.*, 1974, 233.
9 A. P. Terentev and V. M. Potapov, *Zh. Obsch. Khim.*, 1958, **28**, 1161; H.E. Smith, S. C. Cook and M. E. Warren, *J. Org. Chem.*, 1964, **29**, 2265; H. Nozaki, H. Takaya, S. Moriuti and R. Noyori, *Tetrahedron Lett.*, 1966, 5239; R. Noyori, H. Takaya, Y. Nakanishi and H. Nozaki, *Can. J. Chem.*, 1969, **47**, 1242.

10 SHELXTL PLUS, A Program for Crystal Structure Determination, Release 4.11/V, Siemens Analytical X-ray Instruments, Madison, WI, 1990.
11 D. Rogers, *Acta Crystallogr., Sect. A*, 1981, **37**, 734.
12 *International Tables for X-Ray Crystallography*, Kynoch Press, Birmingham, 1974, vol. 4.
13 C. K. Johnson, ORTEP II, Report ORNL 5138, Oak Ridge National Laboratory, Oak Ridge, TN, 1976.
14 R. S. Cahn, C. K. Ingold and V. Prelog, *Angew. Chem.*, 1966, **78**, 413; *Angew. Chem., Int. Ed. Engl.*, 1966, **5**, 385; C. Lecomte, Y. Dusausoy, J. Protas and J. Tirouflet, *J. Organomet. Chem.*, 1974, **73**, 67; K. Stanley and M. C. Baird, *J. Am. Chem. Soc.*, 1975, **97**, 6599.
15 E. L. Eliel, S. H. Wilen and L. N. Mander, *Stereochemistry of Organic Compounds*, Wiley-Interscience, New York, 1994, pp. 365–374.
16 W. S. Sheldrick and S. Heeb, *Inorg. Chim. Acta*, 1990, **168**, 93; R. Krämer, K. Polborn, H. Wanjek, I. Zahn and W. Beck, *Chem. Ber.*, 1990, **123**, 767.
17 D. F. Dersnah and M. C. Baird, *J. Organomet. Chem.*, 1977, **127**, C55.
18 N. L. Allinger and D. Y. Chung, *J. Am. Chem. Soc.*, 1976, **98**, 6798; M. Charton and I. Motoc, *Top. Curr. Chem.*, 1983, **114**, 1.
19 H. Brunner, *Angew. Chem.*, 1983, **95**, 921; *Angew. Chem., Int. Ed. Engl.*, 1983, **22**, 897.
20 C. A. Hunter and J. K. M. Sanders, *J. Am. Chem. Soc.*, 1990, **112**, 5525; C. A. Hunter, J. Singh and J. M. Thornton, *J. Mol. Biol.*, 1991, **218**, 837.
21 D. Armspach, P. R. Ashton, C. P. Moore, N. Spencer, J. F. Stoddart, T. J. Wear and D. J. Williams, *Angew. Chem.*, 1993, **105**, 944; *Angew. Chem., Int. Ed. Engl.*, 1993, **32**, 854.
22 H. G. Schmid, H. Friebolin, S. Kabuß and R. Mecke, *Spectrochim. Acta*, 1966, **22**, 623, H. Friebolin, H. G. Schmid, S. Kabuß and W. Faißt, *Org. Magn. Reson.*, 1969, **1**, 147; A. Jaeschke, H. Muensch, H. G. Schmid, H. Friebolin and A. Mannschreck, *J. Mol. Spectrosc.*, 1969, **31**, 14.
23 M. A. Bennett, G. B. Robertson and A. K. Smith, *J. Organomet. Chem.*, 1972, **43**, C41.
24 W. D. Jones and F. J. Feher, *Inorg. Chem.*, 1984, **23**, 2376; J. A. S. Howell, M. G. Palin, P. McArdle, D. Cunningham, Z. Goldschmidt, H. E. Gottlieb and D. Hezroni-Langerman, *Inorg. Chem.*, 1993, **32**, 3493; *Organometallics*, 1993, **12**, 1694; J. A. Chudek, G. Hunter, R. L. MacKay, P. Kremminger, K. Schlögl and W. Weissensteiner, *J. Chem. Soc., Dalton Trans.*, 1990, 2001; S. E. G. Davies, A. E. Derome and J. P. McNally, *J. Am. Chem. Soc.*, 1991, **113**, 2854; J. W. Faller and K. J. Chase, *Organometallics*, 1995, **14**, 1592.
25 M. A. Dewey, D. A. Knight, A. M. Arif and J. A. Gladysz, *Z. Naturforsch., Teil B.*, 1992, **47**, 1175.
26 C. K. Chou, D. L. Miles, R. Bau and T. C. Flood, *J. Am. Chem. Soc.*, 1978, **100**, 7271.

Received 2*nd October* 1995; *Paper* 5/06474K